
HUMAN-CENTERED BENCHMARKING OF DRIVER MONITORING MODELS

Ruben Dario Florez-Zela

Universidad Nacional de San Agustín de Arequipa (UNSA)
Arequipa, Peru
rflorezz@unsa.edu.pe

ABSTRACT

Vision-based driver monitoring systems are increasingly deployed in safety-critical intelligent transportation settings, yet they are almost always compared on classification accuracy alone. This paper argues that accuracy is insufficient to characterize a model’s fitness for real-world deployment, and proposes the Human-Centered Benchmarking Framework (HCBF), which evaluates models across four dimensions: accuracy, explainability, efficiency, and robustness. The framework is applied to four representative lightweight architectures, MobileNetV3, ShuffleNetV2, EfficientNet-B0, and DeiT-Tiny, on the MRL Eye Dataset for eye-state classification. While the models are nearly indistinguishable on clean-set accuracy, each leads in exactly one dimension, and all four lie on the Pareto frontier. A Human-Centered Score computed under three deployment-oriented weighting scenarios ranks ShuffleNetV2 first throughout. However, this aggregate winner retains less than half of its performance under sensor noise and fails by classifying closed eyes as open, whereas the transformer remains robust. These findings show that aggregate ranking can mask dimension-specific vulnerabilities that are operationally decisive, underscoring the value of multi-dimensional, human-centered evaluation.

Keywords Driver monitoring · Explainable AI · Edge computing · Model robustness · Benchmarking · Intelligent transportation systems.

1 Introduction

Road traffic accidents remain one of the most preventable public health crises today, and driver fatigue sits near its center. A study by the AAA Foundation estimated that roughly 17.6% of fatal crashes in the United States between 2017 and 2021 involved a drowsy driver, about 30,000 fatalities [1]. This figure is widely considered an undercount, since fatigue is difficult to confirm after a crash [2]. What makes drowsiness dangerous is that it erodes reaction time and awareness in ways invisible to the driver until it is too late.

Vision-based Driver Monitoring Systems (DMS) are a promising countermeasure: cameras are non-intrusive, already present in modern cabins, and capture cues such as eye closure and head posture without any wearable sensor [3]. Deep learning has pushed accuracy above 95% on standard eye-state and drowsiness benchmarks [4, 5], and regulation such as the European Union requirement for driver drowsiness and attention warning systems in new vehicle types [6] has fueled optimism about deploying DMS at scale. Yet a gap persists between benchmark accuracy and real-world deployability. A model reaching 98% on a clean dataset may degrade sharply under the lighting changes, occlusion, and sensor noise of an actual cabin, and one that predicts without interpretable justification offers little basis for the human oversight that high-stakes AI requires [7]. Standards such as the EU AI Act and ISO 21448 SOTIF call for transparency and robustness, yet most DMS research still optimizes for a single number: accuracy [3]. Explainability, efficiency, and robustness are mentioned informally rather than measured, leaving a practitioner who must pick an architecture for an embedded platform such as the NVIDIA Jetson Nano without a way to weigh interpretability, robustness under degradation, and real-time latency together. No existing benchmarking framework for driver monitoring appears to address these questions jointly.

This paper proposes the **Human-Centered Benchmarking Framework (HCBF)**, which evaluates vision-based DMS models across four dimensions reflecting the real demands of intelligent transportation: *Accuracy*, *Explainability*, *Efficiency*, and *Robustness*. The framework is demonstrated on four lightweight architectures on the MRL Eye Dataset [8]: MobileNetV3 [9], ShuffleNetV2 [10], EfficientNet-B0 [11], and DeiT-Tiny [12]. Explainability is quantified with deletion and insertion AUC, robustness under Gaussian noise, brightness shifts, and motion blur, and a Human-Centered Score (HCS) computed under three deployment scenarios tests whether rankings hold across stakeholder priorities. The main contributions are:

- A formal Human-Centered Benchmarking Framework (HCBF) extending driver monitoring evaluation beyond accuracy to four operationalized, human-relevant dimensions.
- A quantitative explainability assessment using deletion and insertion AUC, with representative saliency visualizations.
- A multi-criteria analysis combining Pareto frontier identification with a three-scenario Human-Centered Score.
- A failure case analysis showing how and when each architecture degrades, with concrete guidance for safety-critical ITS deployment.

2 Related Work

Vision-based drowsiness detection has evolved from handcrafted indicators such as the Eye Aspect Ratio and PERCLOS, which are inexpensive and interpretable but sensitive to lighting and subject variability [13, 14], to deep learning models that learn features directly from images. CNN- and transformer-based approaches have reported high accuracy on eye-state tasks [4], including MediaPipe-based eye-region classification above 99% [15], embedded visual drowsiness detection on the NVIDIA Jetson Nano [16], and transformer models exceeding 99% on the MRL Eye Dataset [4]. However, recent assessments of driver monitoring systems highlight a persistent gap between reported accuracy and deployment requirements, particularly robustness and interpretable outputs [3].

Real deployment also requires models that balance accuracy with memory, computation, and latency constraints. MobileNetV3 [9], ShuffleNetV2 [10], and EfficientNet-B0 [11] represent efficient CNN design families, while DeiT-Tiny [12] provides a compact transformer alternative based on patch-wise self-attention. Together, these architectures span the main CNN-versus-transformer and accuracy-versus-efficiency choices relevant to embedded vision systems.

Explainability matters in safety-critical settings because accuracy gives no guarantee that a model relies on the correct evidence [17]. Grad-CAM [17] yields qualitative heatmaps that are not comparable across architectures; Petsiuk et al. [18] addressed this with deletion and insertion, whose area under the confidence curve gives a scalar, architecture-agnostic measure well suited to benchmarking. A growing literature urges this shift toward quantitative evaluation [19], and human-centered perspectives stress that explanations must serve the people who depend on the system [7]. Yet across this literature models are still compared almost entirely on accuracy, with explainability, efficiency, and robustness treated as secondary, and no framework integrates all four in a principled, reproducible way for driver monitoring. The HCBF closes that gap with concrete metrics per dimension, applied consistently across four architectures, plus a multi-criteria analysis for deployment decisions under different priorities.

3 Human-Centered Benchmarking Framework

3.1 Framework Overview

The HCBF evaluates vision-based driver monitoring models across four dimensions that reflect the demands of safety-critical intelligent transportation: accuracy, explainability, efficiency, and robustness. Its premise is that accuracy, while necessary, is not sufficient where failures carry physical consequences and human oversight is required [7, 19]. Given candidate models $\mathcal{M} = \{M_1, \dots, M_k\}$ and a dataset \mathcal{D} , the HCBF assigns each M_i a four-dimensional profile

$$\text{HCBF}(M_i) = (\alpha_i, \varepsilon_i, \eta_i, \rho_i), \quad (1)$$

with $\alpha_i, \varepsilon_i, \eta_i, \rho_i$ the accuracy, explainability, efficiency, and robustness scores defined below (Figure 1).

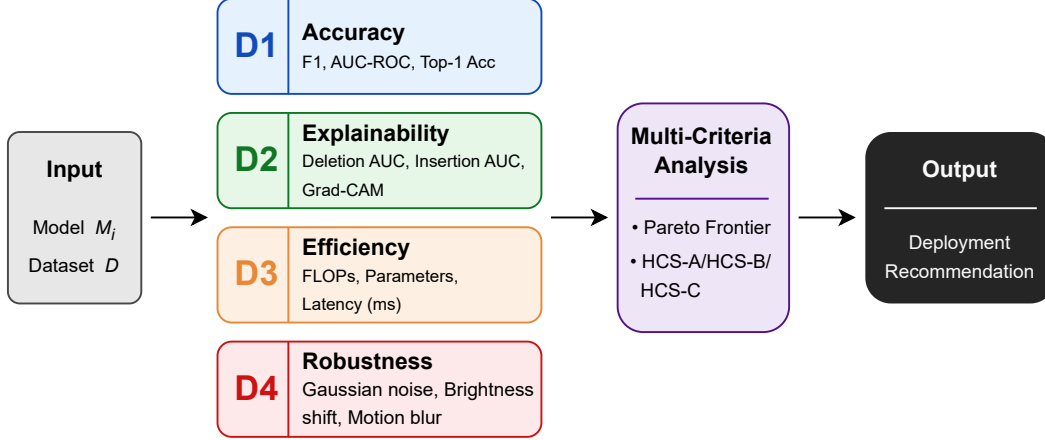


Figure 1: Overview of the Human-Centered Benchmarking Framework (HCBF).

3.2 Dimension 1: Accuracy

Accuracy is measured on the held-out test set through Top-1 accuracy, macro F1-score (robust to class imbalance), and AUC-ROC (threshold-independent), each normalized to $[0, 1]$ and averaged:

$$\alpha_i = \frac{1}{3} (\text{Acc}_i + \text{F1}_i + \text{AUC}_i). \quad (2)$$

3.3 Dimension 2: Explainability

Saliency maps are subjective and not comparable across architectures [19], so the HCBF uses the deletion and insertion metrics of Petsiuk et al. [18], with Grad-CAM [17] for qualitative illustration. Deletion AUC (Del) is the area under the confidence curve as important pixels are masked (lower is better); Insertion AUC (Ins) measures the curve as they are restored (higher is better). The composite aligns both so higher is better:

$$\varepsilon_i = \frac{1}{2} ((1 - \text{Del}_i) + \text{Ins}_i). \quad (3)$$

Attribution maps use Captum on 500 random test images per model.

3.4 Dimension 3: Efficiency

Efficiency uses three measures: parameter count P_i (millions), FLOPs F_i (G, at 224×224), and CPU latency L_i (ms, mean over 1,000 runs, the worst-case scenario without a GPU). Each is min-max normalized across models and combined so higher means more efficient:

$$\eta_i = 1 - \frac{1}{3} \left(\frac{P_i - P_{\min}}{P_{\max} - P_{\min}} + \frac{F_i - F_{\min}}{F_{\max} - F_{\min}} + \frac{L_i - L_{\min}}{L_{\max} - L_{\min}} \right). \quad (4)$$

3.5 Dimension 4: Robustness

Real driving brings conditions absent from clean benchmarks: variable lighting, blur, and sensor noise. Robustness measures how well a model holds accuracy under perturbation [7]. Three types are applied to the test set at three severities each: Gaussian noise ($\sigma \in \{10, 25, 40\}$), brightness scaling (factors $\{0.5, 0.7, 1.5\}$), and horizontal motion blur (kernels $\{5, 11, 17\}$). Let $F1_{i,t,s}$ be the macro F1-score under perturbation type t and severity s . The score is the mean retention relative to the clean baseline:

$$\rho_i = \frac{1}{|\mathcal{T}| \cdot |\mathcal{S}|} \sum_{t \in \mathcal{T}} \sum_{s \in \mathcal{S}} \frac{F1_{i,t,s}}{F1_{i,\text{clean}}}, \quad (5)$$

with $\mathcal{T} = \{\text{noise, brightness, blur}\}$ and $\mathcal{S} = \{\text{mild, moderate, severe}\}$.

3.6 Multi-Criteria Analysis and Human-Centered Score

A Pareto analysis identifies models not dominated on all four dimensions at once: M_i is dominated by M_j if M_j is at least as good on all four and strictly better on one. As a complementary aggregation, the Human-Centered Score collapses a profile into a scalar,

$$\text{HCS}_i = w_\alpha \alpha_i + w_\varepsilon \varepsilon_i + w_\eta \eta_i + w_\rho \rho_i, \quad \sum w = 1. \tag{6}$$

Rather than one fixed weighting, three deployment scenarios (Table 1) follow safety-critical principles [7]: safety-oriented prioritizes robustness and accuracy, deployment-oriented weights efficiency, and balanced treats all equally. The key point is the stability of the ranking across scenarios: a model first under all three is robust to stakeholder preferences, while disagreements reveal genuinely context-dependent cases.

Table 1: Human-Centered Score (HCS) weighting scenarios.

Scenario	w_α	w_ε	w_η	w_ρ	Context
HCS-A (Safety)	0.30	0.20	0.20	0.30	High-risk ADAS
HCS-B (Deployment)	0.25	0.20	0.35	0.20	Edge hardware
HCS-C (Balanced)	0.25	0.25	0.25	0.25	Neutral reference

4 Experimental Setup

4.1 Dataset

All experiments use the MRL Eye Dataset [8], a large-scale collection of infrared eye images from VSB-Technical University of Ostrava, with images from 37 subjects (33 male, 4 female) captured by three infrared sensors under good and poor lighting, with and without glasses. Each image is annotated with subject, gender, glasses, eye state, reflection level, and lighting; the binary eye-state label is used, which maps directly to the open and closed categories relevant to PERCLOS-based monitoring. The split is performed at the subject level (Table 2), so no subject in training appears in validation or test, reflecting the realistic need to generalize to unseen individuals that a random image-level split would overestimate. All images are resized to 224×224 .

Table 2: MRL Eye Dataset composition and subject-level split.

Split	Subjects	Open	Closed	Total
Training	26	38,658	31,893	70,551
Validation	6	2,945	2,025	4,970
Test	5	1,349	8,028	9,377
Total	37	42,952	41,946	84,898

4.2 Models

Four lightweight architectures are benchmarked, spanning distinct designs: MobileNetV3-Large [9] (4.2M parameters), ShuffleNetV2 x1.0 [10] (1.3M, the smallest), EfficientNet-B0 [11] (4.0M, accuracy baseline), and the transformer DeiT-Tiny [12] (5.5M). All use ImageNet-1K pretrained weights with the final head replaced by a two-neuron linear layer for the binary task, covering three CNN designs plus a transformer under equivalent efficiency constraints.

4.3 Training and Evaluation Protocol

Fine-tuning runs in two stages: the head is trained alone for five epochs with the backbone frozen, then all layers jointly, using AdamW [20] ($\text{lr} = 1 \times 10^{-4}$, weight decay 1×10^{-2} , cosine annealing to 1×10^{-6}) for up to 30 epochs with early stopping on validation macro F1 (patience 5) and batch size 32. Augmentation includes horizontal flipping, rotation within $\pm 10^\circ$, brightness and contrast jitter in $[0.8, 1.2]$, and random grayscale ($p = 0.1$); at test time only resizing and ImageNet normalization apply. Experiments run in PyTorch 2.1 with Captum [21], thop [22], and OpenCV, under a fixed seed (42).

Accuracy is computed on the held-out test set, which is never used during training or model selection. Explainability is evaluated with GradientShap maps from Captum on 500 random test images per model to compute deletion and insertion

AUC, while Grad-CAM is used only for qualitative illustration. For robustness, the nine perturbation conditions are applied to the full test set of 9,377 images, yielding nine measurements per model and 36 in total, aggregated into ρ_i via Equation 5. All results follow a single-run protocol with a fixed seed, pretrained initialization, and fixed test set; the full code is publicly available at <https://github.com/rubendflorezzela/hcbf-driver-monitoring>.

5 Results and Failure Case Analysis

This section reports the four HCBF dimensions per model, then a failure case analysis; the aggregation is deferred to Section 6.

5.1 Accuracy and Explainability

On the clean test set all four models perform almost indistinguishably (Table 3, left): composite accuracy α spans only 0.978 to 0.989, MobileNetV3-Large highest and DeiT-Tiny close behind. From an accuracy-only view they would seem interchangeable, which is exactly where a single metric fails to guide a decision. Explainability differs sharply (Table 3, right): EfficientNet-B0 gives by far the most faithful explanations ($\varepsilon = 0.754$), driven by its low deletion AUC of 0.453, while the others cluster near 0.56 to 0.61. Notably, the most accurate model gives the least faithful explanations, already showing the dimensions are independent.

Table 3: Accuracy and explainability results on the test set.

Model	Accuracy				Explainability		
	Top-1	F1	AUC	α	Del↓	Ins↑	ε
MobileNetV3-Large	0.990	0.979	0.999	0.989	0.857	0.978	0.560
ShuffleNetV2 x1.0	0.979	0.957	0.998	0.978	0.778	0.990	0.606
EfficientNet-B0	0.982	0.962	0.995	0.980	0.453	0.961	0.754
DeiT-Tiny	0.988	0.975	0.998	0.987	0.772	0.985	0.606

5.2 Efficiency

ShuffleNetV2 is most efficient on all three raw measures, taking the maximum score (Table 4): at 1.26M parameters and 0.152 GFLOPs it is about four times smaller than MobileNetV3-Large and EfficientNet-B0. DeiT-Tiny, though competitive in latency, costs 1.075 GFLOPs (roughly seven times ShuffleNetV2), the expected price of self-attention, leaving it last ($\eta = 0.287$).

Table 4: Efficiency results; η is the normalized score (higher is better).

Model	Params (M)	FLOPs (G)	Latency (ms)	η
MobileNetV3-Large	4.20	0.234	11.76	0.710
ShuffleNetV2 x1.0	1.26	0.152	11.33	1.000
EfficientNet-B0	4.01	0.414	16.55	0.354
DeiT-Tiny	5.48	1.075	12.06	0.287

5.3 Robustness

Robustness shows the sharpest split (Table 5). All models tolerate brightness and blur well (above 0.94 retention), but under Gaussian noise the three CNNs collapse to 27 to 48% retention while DeiT-Tiny holds 92%. EfficientNet-B0 is the most fragile (0.268), despite leading explainability. This single perturbation drives the whole ranking, giving DeiT-Tiny the top score ($\rho = 0.959$) almost entirely through noise resilience. The pattern is consistent with reports that well pre-trained transformers resist perturbations better than comparable CNNs [23], and it matters here because Gaussian noise models the sensor noise of low-cost infrared cameras in poor lighting, conditions present across much of the dataset.

Table 5: Robustness results as mean F1 retention per perturbation type.

Model	Gaussian noise	Brightness	Motion blur	ρ
MobileNetV3-Large	0.466	1.000	0.946	0.804
ShuffleNetV2 x1.0	0.484	1.007	0.967	0.819
EfficientNet-B0	0.268	0.989	0.993	0.750
DeiT-Tiny	0.923	0.977	0.978	0.959

5.4 Failure Case Analysis

To understand the CNN collapse, the perturbed inputs and saliency maps were examined at severe noise ($\sigma = 40$); Figure 2 shows examples whose label is *closed*. Three points stand out. The noise does not destroy semantic content: the eyelid contour stays visible to a human, so the errors are not from lost information. The failure is systematic, with the CNNs flipping closed eyes to *open*, the more dangerous error here since a drowsy driver is read as alert. The CNN saliency maps become diffuse and lose clear focus on the eyelid region, consistent with their unstable predictions under noise. By contrast, DeiT-Tiny preserves the correct classification across the same examples, even though its attribution map is less visually pronounced. A benchmark on clean accuracy alone would rank all four as near-equivalent and never warn that three models fail catastrophically, in the more hazardous direction, under a perturbation that is realistic and visually mild.

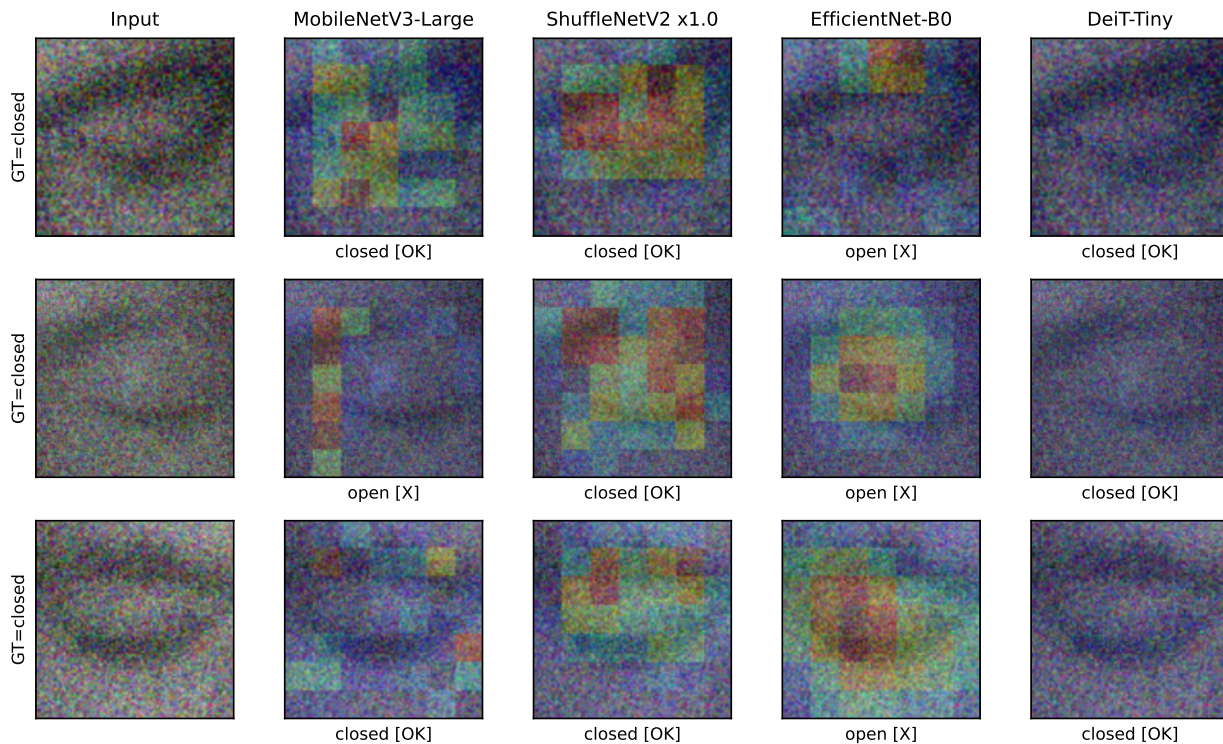


Figure 2: Saliency maps under severe Gaussian noise ($\sigma = 40$); label is *closed*. CNN columns use Grad-CAM, while DeiT-Tiny uses GradientShap attribution.

6 Multi-Criteria Analysis: Pareto Frontier and Human-Centered Score

The per-dimension results show no single architecture is best on all four criteria. They are now consolidated into the HCBF profiles, the Pareto frontier is identified, and the HCS is computed under the three scenarios of Section 3.

6.1 Profiles and Pareto Frontier

Table 6 presents the complete normalized profile of each model, and Figure 3 visualizes these profiles as a radar chart.

A striking pattern emerges from Table 6: each model leads in exactly one dimension and no other, MobileNetV3-Large in accuracy (0.989), EfficientNet-B0 in explainability (0.754), ShuffleNetV2 in efficiency (1.000), and DeiT-Tiny in robustness (0.959). This clean separation is the empirical core of the study: choosing an architecture is not about finding one superior model but about deciding which dimension matters most. A direct consequence is that all four are Pareto-non-dominated, since a model cannot be dominated if it is the unique best on at least one axis, so the Pareto frontier is the entire set. From a multi-objective standpoint this is the most informative outcome possible: the choice cannot be made on technical grounds alone and must follow the priorities of the application, which the HCS formalizes.

Table 6: Normalized HCBF profiles (best per column in bold).

Model	α (Acc)	ε (Expl)	η (Eff)	ρ (Rob)
MobileNetV3-Large	0.989	0.560	0.710	0.804
ShuffleNetV2 x1.0	0.978	0.606	1.000	0.819
EfficientNet-B0	0.980	0.754	0.354	0.750
DeiT-Tiny	0.987	0.606	0.287	0.959

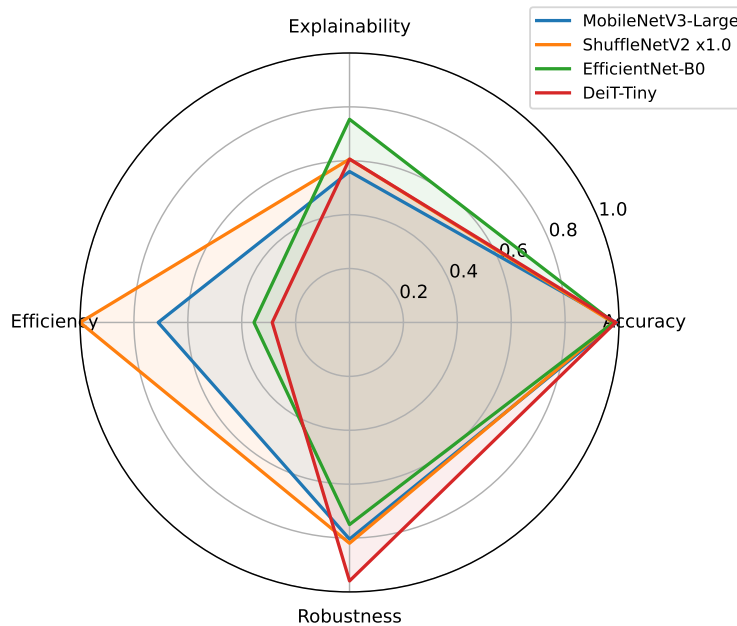


Figure 3: Radar chart of the HCBF profiles.

6.2 Human-Centered Score Across Scenarios

Table 7 reports the HCS and rank per scenario. ShuffleNetV2 ranks first in all three and MobileNetV3-Large second in all three, so the top of the ranking is independent of how the criteria are weighted: ShuffleNetV2 pairs perfect efficiency with accuracy and robustness high enough to avoid penalization, and its score even rises under the deployment scenario (HCS-B). The lower half is less stable, as EfficientNet-B0 and DeiT-Tiny swap third and fourth depending on whether explainability or robustness is valued more, exactly the context-dependence the multi-scenario design reveals and an argument against any single fixed-weight score.

Table 7: Human-Centered Score per scenario (rank in parentheses).

Model	HCS-A (Safety)	HCS-B (Deploy.)	HCS-C (Balanced)
MobileNetV3-Large	0.7920 (2)	0.7687 (2)	0.7659 (2)
ShuffleNetV2 x1.0	0.8604 (1)	0.8795 (1)	0.8508 (1)
EfficientNet-B0	0.7407 (4)	0.6698 (3)	0.7096 (4)
DeiT-Tiny	0.7625 (3)	0.6603 (4)	0.7099 (3)

7 Discussion and Conclusion

This paper introduced the Human-Centered Benchmarking Framework (HCBF), which evaluates vision-based driver monitoring models across four dimensions reflecting the demands of safety-critical intelligent transportation: accuracy, explainability, efficiency, and robustness. Its contribution is not a new architecture but a way of evaluating existing ones that moves past the single-metric comparisons dominating the field. Applied to four lightweight architectures on the MRL Eye Dataset, the framework showed that each model leads in a different HCBF dimension, placing all four on the Pareto frontier. Therefore, model selection must depend on deployment priorities rather than accuracy alone. The most consequential finding is the dissociation between aggregate ranking and dimension-specific safety. ShuffleNetV2, the HCS winner across all three scenarios and the obvious pick on a conventional accuracy-and-efficiency basis, retains less than half of its clean performance under Gaussian noise and fails by classifying closed eyes as open, the exact failure a drowsiness detector exists to prevent, while DeiT-Tiny stays robust but ranks lower for its cost. This matters because real deployment is far less benign than a clean benchmark: European requirements for driver drowsiness and attention warning systems have applied to new vehicle types since July 2024 [6], placing these systems on automotive hardware where low-cost infrared cameras in poor lighting can produce the kind of sensor noise that collapsed the CNNs here. The HCBF makes that vulnerability visible at the point of decision, so a designer targeting low-cost sensors would weight robustness heavily or treat it as a hard constraint, making DeiT-Tiny the preferred choice despite its cost. This advantage is consistent with reports that well pre-trained transformers resist perturbations better than comparable CNNs [23], and the failure maps suggest the CNNs’ local receptive fields are disrupted by high-frequency noise while global self-attention is not.

Several limitations qualify these findings and define the next steps: a single dataset and four architectures; a robustness analysis without occlusion, compression, or adversarial perturbations; explainability measured by attribution faithfulness rather than usefulness to a human operator; and latency measured on a desktop CPU as an embedded proxy. The natural extensions are cross-dataset evaluation, direct profiling on the NVIDIA Jetson Nano, broader perturbations, and a user study of explanation usefulness. The framework is task-agnostic, applying unchanged to problems such as yawning detection, gaze estimation, and head pose estimation, and to any safety-critical vision task where silent failures are costly. The HCBF aims to encourage a practice in which interpretability, deployability, and trustworthiness are evaluated jointly with accuracy, not as afterthoughts.

References

- [1] AAA Foundation for Traffic Safety. Drowsy driving in fatal crashes, united states, 2017–2021. <https://aaaafoundation.org/research/drowsy-driving-in-fatal-crashes-united-states-2017-2021/>, 2024. Accessed: March 2026.
- [2] National Highway Traffic Safety Administration. Traffic safety facts: Drowsy driving. <https://www.nhtsa.gov/risky-driving/drowsy-driving>, 2023. Accessed: March 2026.
- [3] Guangwei Yang, Christie Ridgeway, Andrew Miller, and Abhijit Sarkar. Comprehensive assessment of artificial intelligence tools for driver monitoring and analyzing safety critical events in vehicles. *Sensors*, 24(8):2478, 2024.
- [4] Osama F Hassan, Ahmed F Ibrahim, Ahmed Gomaa, MA Makhlof, and B Hafiz. Real-time driver drowsiness detection using transformer architectures: a novel deep learning approach. *Scientific Reports*, 15(1):17493, 2025.
- [5] Tahesin Samira Delwar et al. AI-and deep learning-powered driver drowsiness detection method using facial analysis. *Applied Sciences*, 15(3):1102, 2025.
- [6] European Parliament and Council. Regulation (EU) 2019/2144 on type-approval requirements for motor vehicles and their trailers. <https://eur-lex.europa.eu/legal-content/EN/TXT/?uri=CELEX:32019R2144>, 2019. Drowsiness detection mandate applicable from July 2024.
- [7] Dominik Kowald et al. Establishing and evaluating trustworthy ai: overview and research challenges. *Frontiers in Big Data*, 7, 2024.
- [8] R. Fusek. Pupil localization using geodesic distance. In *Advances in Visual Computing*, volume 11241 of *Lecture Notes in Computer Science*, pages 433–444. Springer, 2018.
- [9] Andrew Howard et al. Searching for MobileNetV3. In *Proceedings of the IEEE/CVF International Conference on Computer Vision (ICCV)*, pages 1314–1324, 2019.
- [10] Ningning Ma, Xiangyu Zhang, Hai-Tao Zheng, and Jian Sun. ShuffleNet V2: Practical guidelines for efficient CNN architecture design. In *Proceedings of the European Conference on Computer Vision (ECCV)*, pages 116–131, 2018.

- [11] Mingxing Tan and Quoc Le. EfficientNet: Rethinking model scaling for convolutional neural networks. In *Proceedings of the 36th International Conference on Machine Learning (ICML)*, pages 6105–6114, 2019.
- [12] Hugo Touvron et al. Training data-efficient image transformers and distillation through attention. In *Proceedings of the 38th International Conference on Machine Learning (ICML)*, volume 139, pages 10347–10357. PMLR, 2021.
- [13] Gulbadan Sikander and Shahzad Anwar. Driver fatigue detection systems: A review. *IEEE Transactions on Intelligent Transportation Systems*, 20(6):2339–2352, 2018.
- [14] Yaman Albadawi, Maen Takruri, and Mohammed Awad. A review of recent developments in driver drowsiness detection systems. *Sensors*, 22(5):2069, 2022.
- [15] Ruben Florez et al. A CNN-based approach for driver drowsiness detection by real-time eye state identification. *Applied Sciences*, 13(13):7849, 2023.
- [16] Ruben Florez et al. A real-time embedded system for driver drowsiness detection based on visual analysis of the eyes and mouth using convolutional neural network and mouth aspect ratio. *Sensors*, 24(19):6261, 2024.
- [17] Ramprasaath R. Selvaraju et al. Grad-CAM: Visual explanations from deep networks via gradient-based localization. In *Proceedings of the IEEE International Conference on Computer Vision (ICCV)*, pages 618–626, 2017.
- [18] Vitali Petsiuk, Abir Das, and Kate Saenko. RISE: Randomized input sampling for explanation of black-box models. In *Proceedings of the British Machine Vision Conference (BMVC)*, 2018.
- [19] Meike Nauta et al. From anecdotal evidence to quantitative evaluation methods: A systematic review on evaluating explainable AI. *ACM Computing Surveys*, 55(13s):295, 2023.
- [20] Ilya Loshchilov and Frank Hutter. Decoupled weight decay regularization. In *International Conference on Learning Representations (ICLR)*, 2019.
- [21] Narine Kokhlikyan et al. Captum: A unified and generic model interpretability library for PyTorch. arXiv:2009.07896, 2020.
- [22] Ligeng Zhu. thop: PyTorch-OpCounter. <https://github.com/Lyken17/pytorch-OpCounter>, 2023. Accessed: March 2026.
- [23] Srinadh Bhojanapalli et al. Understanding robustness of transformers for image classification. In *Proceedings of the IEEE/CVF International Conference on Computer Vision (ICCV)*, pages 10231–10241, 2021.